Jurnal Teknologi, 43(F) Dis. 2005: 1–13

ON THE EFFECT OF AXIAL DISPERSION IN THE NUMERICAL SIMULATION OF FAST CYCLING ADSORPTION PROCESSES

C. Y. SOO[1], Y. L. LAI[2], T. G. CHUAH[3], S. MUSTAPHA[4] & T. S. Y. CHOONG[5*]

Abstract. The effects of axial dispersion in the numerical simulation of fast cycling adsorption processes were studied. The main objectives are: (1) to re-examine the observation of Alpay [1] on the effect of axial dispersion on the oxygen purity for a 1.0 m column, and (2) to investigate numerically the effect of axial dispersion on the oxygen purity and cycle-averaged feed flow rate of an ultra rapid pressure swing adsorption (URPSA) process, which employed a column of 0.2 m in length. The linear driving force (LDF) model was employed to model the mass transfer within the adsorbent particles. Numerical simulation was carried out by discretising the partial differential equations (PDEs) in the space domain to a system of ordinary differential equations (ODEs), using the method of orthogonal collocation (OC). The ODEs were then integrated using a subroutine from IMSL FORTRAN Library, which is suitable for the integration of stiff ODEs. For Alpay's experimental conditions, unphysical numerical results were observed for an axial dispersion coefficient predicted by Langer's correlation. However, no such numerical difficulties were encountered for an URPSA process. Our numerical simulations showed a reduction of up to 10 percentage points when values of axial dispersions were increased. The axial dispersion was found to have no effect on the cycle-averaged feed gas rate. Future works are deemed necessary to device suitable strategy to overcome the numerical difficulties encountered here.

Keywords: Rapid pressure swing adsorption, modelling, numerical simulation, air separation, axial dispersion

Abstrak. Kesan serakan paksi dalam penyelakuan perangkaan proses penjerapan berkitar pantas telah dikaji. Objektif kajian ini adalah untuk (1) mengkaji semula cerapan Alpay [1] dalam kesan serakan paksi ke atas ketulenan oksigen dalam turus yang panjangnya 1.0 m, dan (2) mengkaji secara perangkaan kesan serakan paksi ke atas ketulenan oksigen dan kadar aliran suapan purata-kitar bagi proses jerapan buaian tekanan ultracepat (URPSA) dalam turus yang panjangnya 0.2 m. Daya pacu linear telah digunakan untuk memodel pemindahan jisim di antara partikel bahan penjerap. Penyelakuan perangkaan telah dijalankan dengan menurunkan persamaan kebezaan separa (PDEs) ke dalam persamaan kebezaan biasa (ODEs) dengan menggunakan kaedah ortogon penempatan bersama (OC). Sistem ODEs itu kemudian dikamil dengan menggunakan subrutin daripada Perpustakaan IMSL FORTRAN, di mana subrutin ini adalah sesuai untuk kamiran ODEs kaku. Untuk keadaan eksperimen Alpay, keputusan penyelakuan yang tidak fizikal telah dicerap untuk serakan paksi yang dijangka oleh kolerasi Langer. Walau bagaimanapun, tiada cerapan sebegini ditemui untuk proses URPSA. Keputusan penyelakuan kami telah menunjukkan satu penurunan sebanyak 10 peratus apabila nilai serakan paksi bertambah. Serakan paksi didapati tiada kesan ke atas kadar aliran suapan

[1,2,3,4&5]Department of Chemical and Environmental Engineering, Universiti Putra Malaysia, 43400 Serdang, Malaysia.
* Corresponding author: Fax: (603)-86567099; E-mail: tsyc2@eng.upm.edu.my

purata-kitar. Kerja masa depan adalah diperlukan untuk mencipta strategi yang sesuai untuk mengatasi kesulitan perangkaan yang telah ditemui.

Kata kunci: Proses jerapan buaian tekanan, permodelan, penyelakuan perangkaan, permisahan udara, serakan paksi

1.0 INTRODUCTION

Rapid pressure swing adsorption (RPSA), originally developed by Turnock and Kadlec [2], employs only a single packed bed, with short cycle times (in the order of seconds) and small particle size (typically 200 to 700 μm in diameter). Compared with conventional pressure swing adsorption (PSA) systems, it has the advantage of process simplicity and higher production rate at equal purity and recovery [3]. An application of RPSA is the enrichment of oxygen from air studied by Alpay [1]. The experimental conditions of Alpay are given in Table 1.

Table 1 Experimental conditions of Alpay [1] and Murray [4]

Operating variable	Description	Unit	Value	
			Alpay	Murray
d_c	bed diameter	m	0.05	0.05
L	bed length	m	1.0	0.2
P_f	feed pressure	bar	1.84	2.0
T	temperature	K	290	290
ε_b	bed porosity		0.35	0.35
ε_p	particle porosity		0.55	0.57
ρ_b	bed bulk density	kg m^{-3}	800	790
H_A	Henry's law constant for oxygen	m^3 kg^{-1}	3.5×10^{-3}	3.5×10^{-3}
H_B	Henry's law constant for nitrogen	m^3 kg^{-1}	7.7×10^{-3}	7.7×10^{-3}
d_p	particle diameter	μm	200	300
$\bar{Q}_p$	product delivery rate		1.0×10^{-5} m^3 s^{-1} @ P_{am}, T_{am}	0.5ℓ min^{-1} at s.t.p.

A basic RPSA cycle consists of two steps: pressurisation and depressurisation, as illustrated in Figure 1. During pressurisation, air is fed to the column through a three-way valve. Pressure increases rapidly at the feed end of the column. As feed air flows down the column, nitrogen is preferentially adsorbed on the zeolite 5A adsorbent, resulting in an oxygen-enriched gas phase.

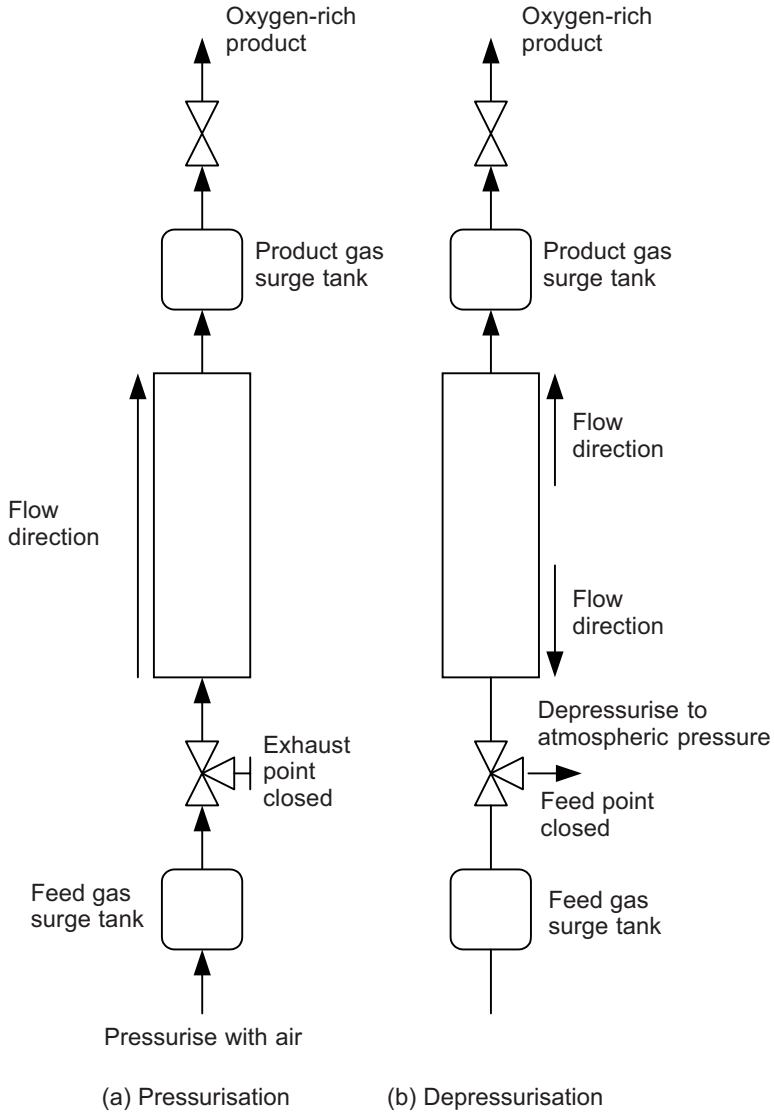

Figure 1 Basic steps in RPSA [5]

In the depressurisation step, the feed valve is closed and the exhaust valve at the feed end is opened to atmospheric pressure, resulting in a rapid pressure drop at the feed end of the column, followed by desorption of the adsorbed nitrogen. The gas leaving the exhaust port is enriched with nitrogen. As there is a pressure maximum in the bed during depressurisation, a pressure gradient is always maintained between this maximum and the product end of the bed, which results in a continuous product stream throughout the cycle.

The adsorbent productivity of a single column PSA can be further improved by reducing further the cycle time and using a shorter bed [4,6,7]. This process is referred here as the ultra rapid pressure swing adsorption (URPSA). Murray [4] has conducted experiments on URPSA using a short bed, L = 0.2 m, and very short cycle times, t_c = 0.2 s – 2.0 s. The experimental conditions of Murray are given in Table 1.

The axially dispersed plug flow (ADPF) model is often used to model the deviation of the actual flow pattern from plug flow in PSA processes. Numerically, the inclusion of axial dispersion in PSA models helps to eliminate the predicted discontinuities of concentration due to shocks [3]. In RPSA, the effect of axial dispersion on CSS oxygen product purity was investigated numerically by Alpay [8]. Increasing the numerical value of the axial dispersion coefficient significantly reduced the predicted oxygen purity by up to 10 percentage points. However, as we have established earlier, the model formulation of Alpay does not conserve mass and may introduce substantial numerical error [5,9]. Therefore, the status of Alpay observation is unclear.

The objectives of this work are: (1) to re-examine the observation of Alpay on the effect of axial dispersion on the oxygen purity, and (2) to investigate numerically the effect of axial dispersion on the oxygen product purity and the cycle-averaged feed flow rate of an URPSA process.

2.0 MATHEMATICAL MODELS

In this work, a cycle always starts at the start of pressurisation and is viewed as complete at the instant of finishing the depressurisation step. A linear driving force (LDF) model was employed to model the mass transfer within the adsorbent particles. We considered a rich, binary gas mixture consisting of oxygen (component A) and nitrogen (component B). The subscript i refers to component i, where $i = A, B$. The assumptions made are:

(1) The ideal gas law is obeyed.
(2) The process is assumed to be isothermal.
(3) The bed is packed uniformly with spherical particles.
(4) The flow pattern is described by the axially dispersed plug flow (ADPF) model with a constant axial dispersion coefficient.
(5) Gas flow is described by Ergun equation.
(6) Adsorption isotherms for both oxygen and nitrogen are given by Henry's Law.
(7) The radial temperature and concentration gradients are negligible.
(8) A step change of pressure at the feed end occurs for both pressurisation and depressurisation steps.
(9) The product delivery rate is constant with time.
(10)) The packed bed is initially in equilibrium with atmospheric air.

The governing equations are:

$$\frac{\partial P}{\partial t} = -\frac{1}{\varepsilon_b}\left\{\frac{\partial (uP)}{\partial z} + \rho_b RT \sum_i \frac{d\overline{q}_i}{dt}\right\} \tag{1}$$

and

$$\frac{\partial y_A}{\partial t} = -\frac{1}{\varepsilon_b P}\left\{\frac{\partial (uPy_A)}{\partial z} - D\frac{\partial}{\partial z}\left(P\frac{\partial y_A}{\partial z}\right) + \rho_b RT\frac{d\overline{q}_A}{dt}\right\} - \frac{y_A}{P}\frac{\partial P}{\partial t} \tag{2}$$

For the process conditions used in this work,

$$\frac{d\overline{q}_i}{dt} = 15\frac{D_{e_i}^*}{r_p^2}\left(q_i^* - \overline{q}_i\right) \tag{3}$$

The gas flows through a packed bed is described by the Ergun equation:

$$\frac{dP}{dz} = -\alpha\frac{\mu(1-\varepsilon_b)^2}{d_p^2\varepsilon_b^3}u - 1.75\frac{(1-\varepsilon_b)\rho_g}{d_p^2\varepsilon_b^3}u^2 \tag{4}$$

The value of the coefficient α = 180 as suggested by McDonald [10] is found to describe accurately the gas flow in a packed bed studied by Alpay [1]. However, Murray [4] suggested that α = 250 described his experiment conditions better.

Two main mechanisms contributed to axial dispersion. These are (i) molecular diffusion and (ii) turbulent mixing arising from the splitting and recombination of flows around adsorbent particles. The correlation proposed by Langer *et al.* [11] can be used here to predict the axial dispersion coefficient:

$$D_{ax} = \tau_{ax}D_m + \frac{ud_p}{Pe_\infty\varepsilon_b\left(1 + \dfrac{\beta_{ax}\tau_{ax}D_m\varepsilon_b}{ud_p}\right)} \tag{5}$$

where Pe_∞ is the limiting value of the Peclet number, β_{ax} is the radial dispersion factor and D_m is the molecular diffusion coefficient. The axial tortuosity factor, τ_{ax}, is given by:

$$\tau_{ax} = 0.45 + 0.55\varepsilon_b \tag{6}$$

The term including $\beta_{ax}\tau_{ax}D_m$ accounts for the perceived effect on axial dispersion due to local radial concentration and velocity gradients. The theoretical value of β_{ax}, 8, is obtained from a highly turbulent random walk model. The value of Pe_∞ depends on the particle size and for $d_p < 3000$ μm is given as:

$$Pe_\infty = 670d_p \tag{7}$$

The detailed derivation of the model and the equations describing the respective boundary conditions for pressurization and depressurization steps can be found in Choong [9].

3.0 NUMERICAL SIMULATION

The partial differential equations (PDEs) in the RPSA model are discretised in the space domain to a system of ordinary differential equations (ODEs) using the orthogonal collocation (OC) method. The ODEs are then integrated over time. All simulations are performed using the OC method with a 20^{th} degree polynomial. Details on the OC method can be found in Rice and Do [12] and Villadsen and Michelson [13]. The computer program is written in FORTRAN 90 for the implementation of modelling and simulation. Standard algorithms from the IMSL FORTRAN library are employed as external subroutines. The ODE integration algorithm employed the IMSL FORTRAN library subroutine DIVPAG, which is based on a variable order, variable step method implementing backward differentiation formulae, and is suitable for a stiff system of first order non-linear ODEs. The accuracy of the integration is controlled by the absolute tolerance, TOL, used in the subroutine. The value of TOL used in the simulation is 1×10^{-5}.

The CSS is calculated using the method of successive substitution. The simulation involves a series of complete cycles with the results of the previous cycle used as initial conditions for the next cycle. The CSS is determined using the rational stopping criterion developed earlier by Choong *et al.* [14].

4.0 RESULTS AND DISCUSSION

As mentioned by Ruthven *et al.* [3], the inclusion of axial dispersion in PSA models helps to eliminate the predicted discontinuities of concentration due to shocks. The axial dispersion coefficient can be estimated using the Langer's correlation or any other suitable correlation. A constant effective axial dispersion coefficient, D, 1×10^{-3} m^2 s^{-1} is often used in the literature for a 1 m length column RPSA [9,15,16]. However, for process conditions used by these researchers, the Langer's correlation estimated D to be around 1×10^{-4} m^2 s^{-1}, not $D = 1 \times 10^{-3}$ m^2 s^{-1}. The effects of these two D are to be investigated here.

For the simulation results based on the experimental conditions of Alpay [1] (Table 1), about 2000 cycles were required to reach CSS, as shown in Figure 2. The oxygen mole fraction profiles did not vary much after 1000 cycles. When the commonly used $D = 1 \times 10^{-3}$ m^2 s^{-1} was applied in the simulation, the oxygen mole fraction waves travelled smoothly down the column, as shown in Figure 2. However, using the Langer's correlation, the results were unphysical as there were oxygen mole fractions exceeding 1.0 in the column, as shown in Figure 3. From a close

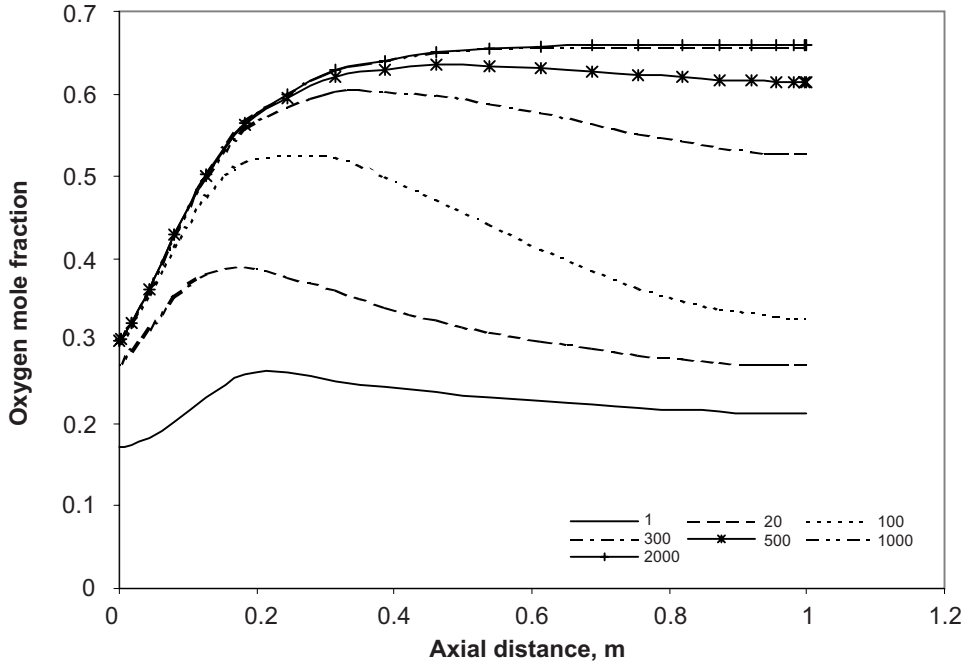

Figure 2 Oxygen mole fraction as a function of axial distance. Process conditions are from Alpay [1] with an effective axial dispersion coefficient, $D = 1 \times 10^{-3}$ m^2 s^{-1}

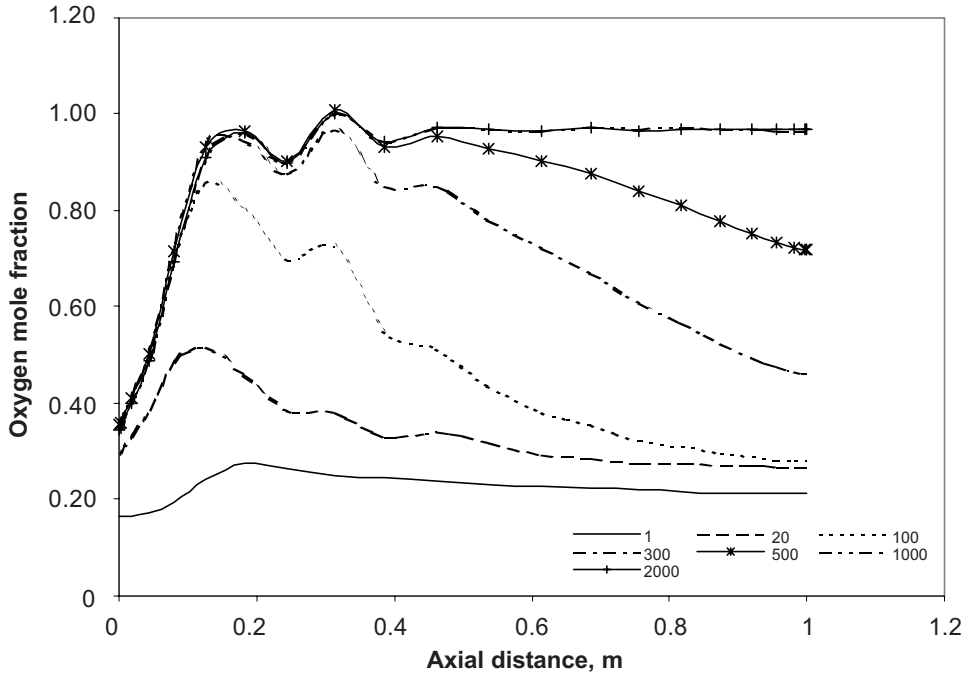

Figure 3 Oxygen mole fraction as a function of axial distance. Process conditions are from Alpay [1] with an effective axial dispersion coefficient, $D = 1 \times 10^{-4}$ m^2 s^{-1}

examination of Figure 3, the oxygen mole fraction waves were accumulated at $z = 0.2$ m and did not travel down the end of column.

The numerical difficulty observed in the 1 m length column was not encountered in simulations using the experimental data of Murray [4] as shown in Table 1. The simulations were performed using the Langer's correlation. The experimental conditions of Murray [4] are similar to Alpay [1], except a shorter column (0.2 m) is used rather than a column length of 1 m. Figure 4 shows the oxygen mole fraction as a function of axial distance for the experimental conditions of Murray [4]. There is no unphysical value of oxygen mole fraction as found in Figure 3. A comparison of the effective axial dispersion profiles and the velocity profiles was made for the respective experimental conditions of Alpay [1] and Murray [4]. Figure 5 shows the effective axial dispersion profiles across the column for the experimental conditions of Alpay [1] and Murray [6]. It is observed that the effective axial dispersions for both experimental conditions are in the same order of magnitude. Figure 6 reveals that the velocity calculated from Murray's experimental conditions is generally higher than that of Alpay's experimental conditions. This allows deeper penetration of the oxygen mole fraction wave for the numerical simulations of Murray's experimental conditions and therefore, no numerical difficulty was encountered.

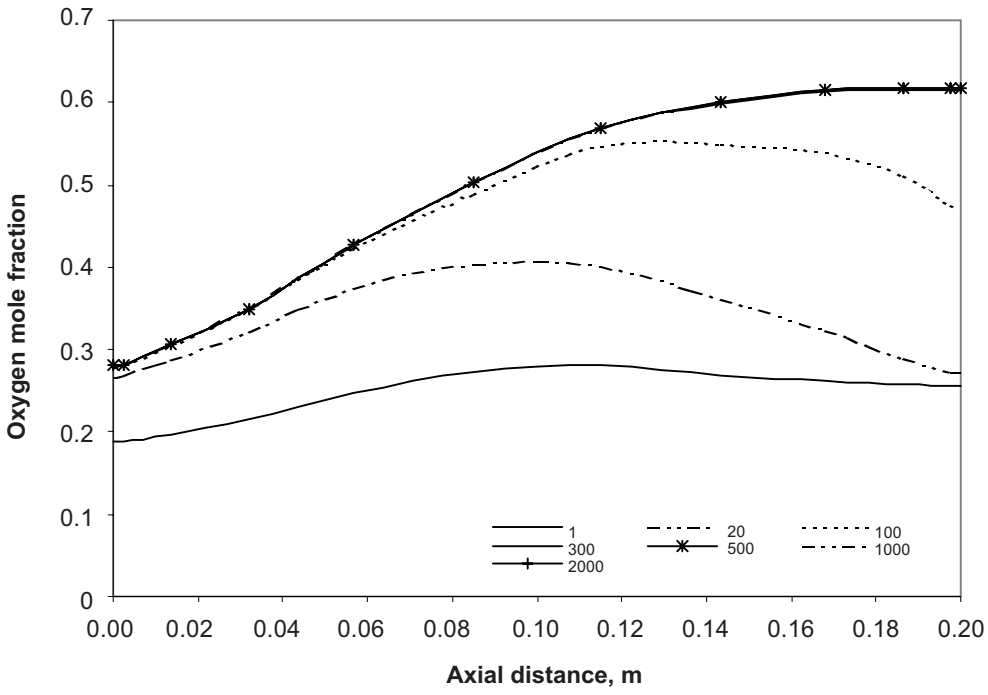

Figure 4 Oxygen mole fraction as a function of axial distance. Process conditions are from Murray [4] with effective axial dispersion coefficient, D = Langer *et al.* [9]

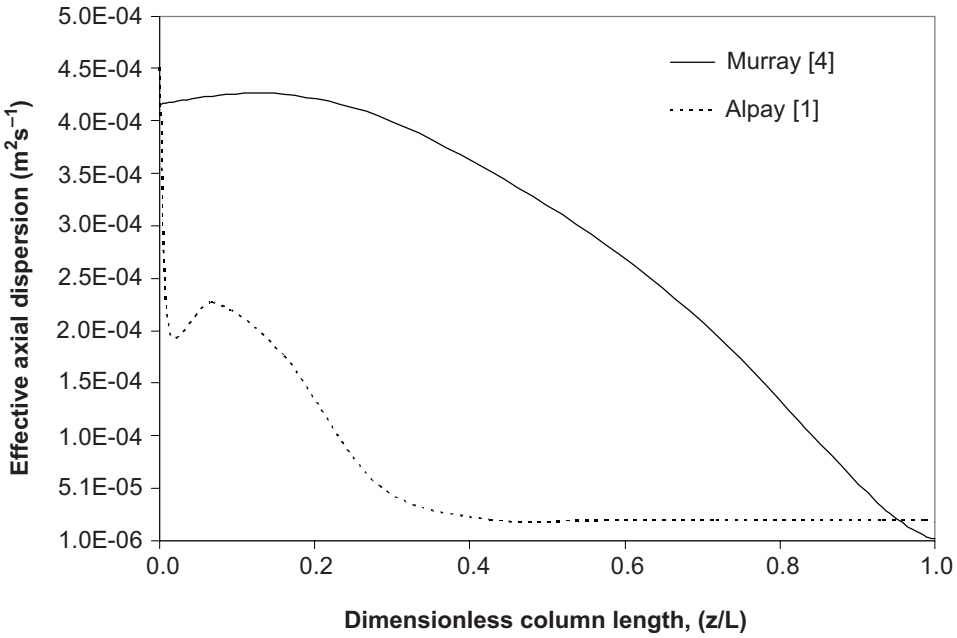

Figure 5 Effective axial dispersion coefficient profiles: comparison of experimental conditions of Alpay [1] and Murray [4]

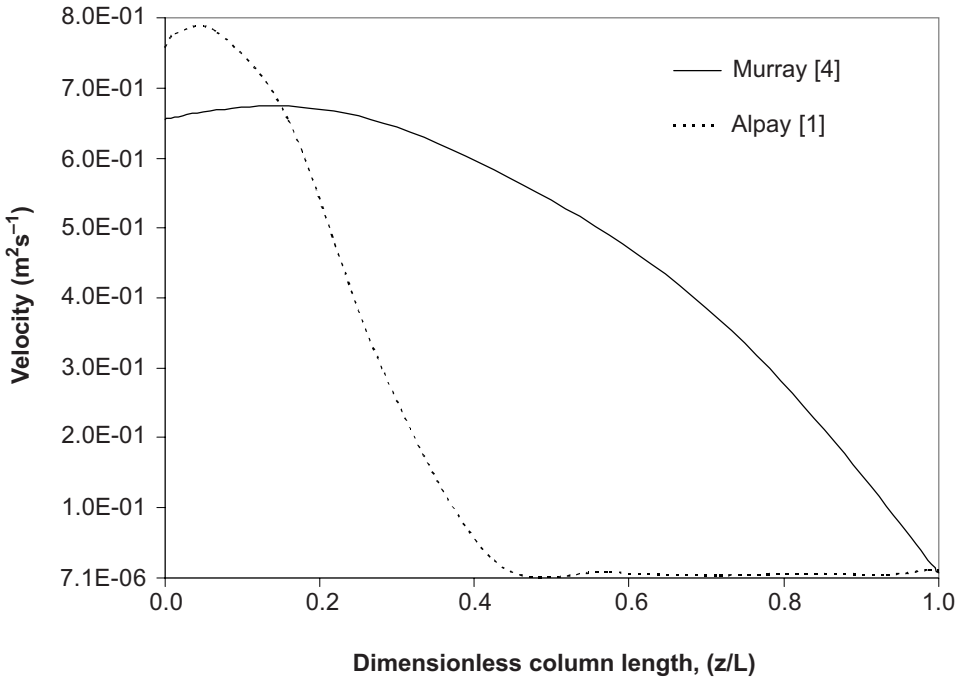

Figure 6 Velocity profiles: comparison of experimental conditions of Alpay [1] and Murray [4].

Having confirmed that there was no numerical difficulty for the simulation of experimental conditions of Murray [4], the effect of axial dispersion on cycle-averaged feed gas rate and oxygen product purity were studied. The two effective axial dispersion coefficients used are: constant $D = 1 \times 10^{-3}$ m^2 s^{-1} and D obtained from the Langer correlation. Figures 7 and 8 show the effect of axial dispersion on oxygen product purity and cycle-averaged feed gas rate, respectively. It is observed that increasing the value of effective axial dispersion coefficient reduces the oxygen product purity. The oxygen product purity was reduced by an average of 8 percentage points. There was a maximum reduction of 10 percentage points in oxygen product purity when $D = 1 \times 10^{-3}$ m^2 s^{-1} was used. However, Figure 8 shows that the effective axial dispersion coefficients have no effect on the cycle-averaged feed gas rates. This is because our model does not imply axial dispersion of total material. From Figure 7, we may conclude that the optimum cycle time for oxygen product purity is 1.0 s.

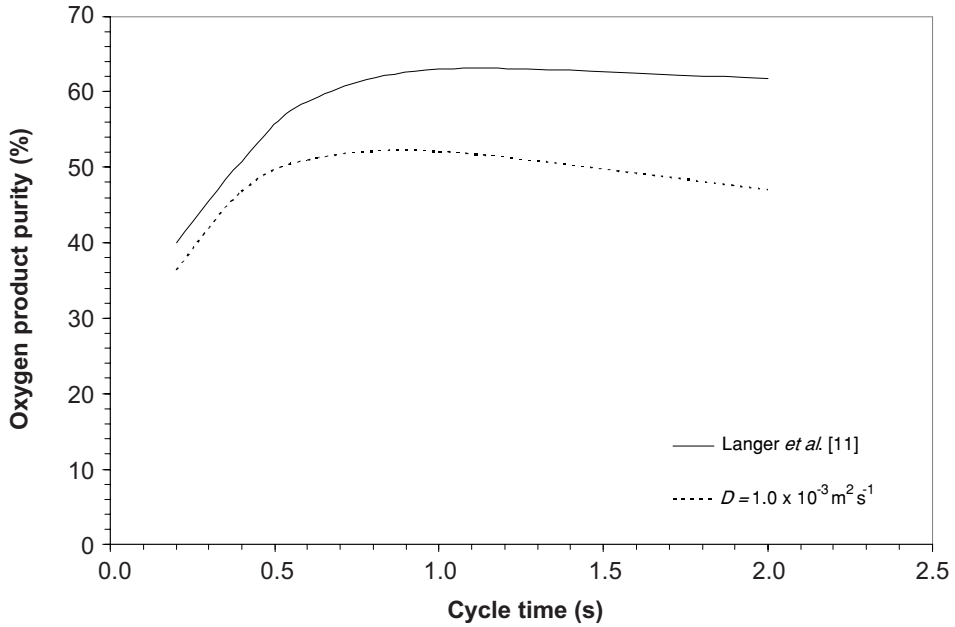

Figure 7 Effect of axial dispersion on oxygen product purity as a function of cycle time. Process conditions are from Murray [4]

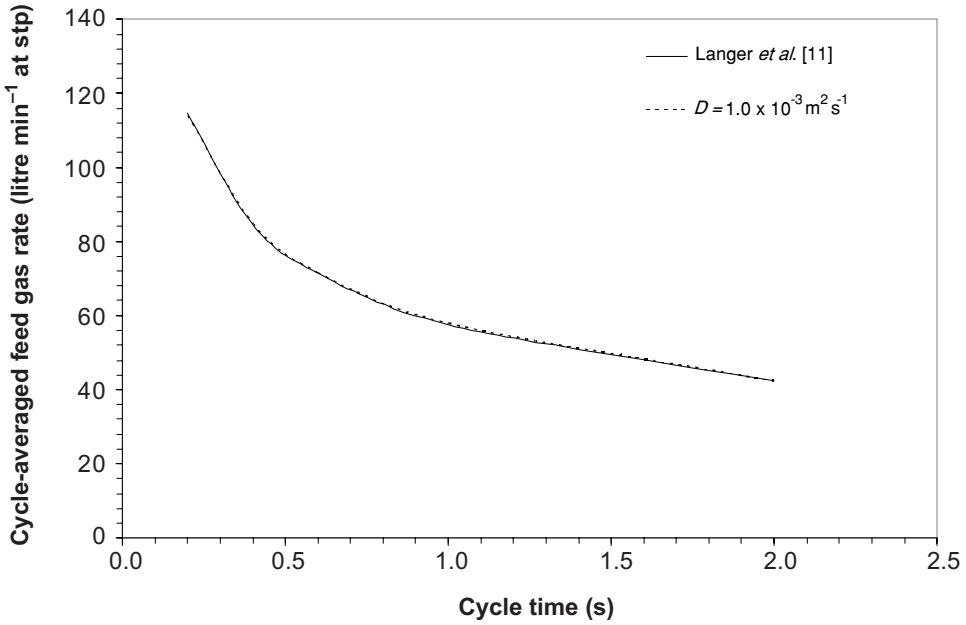

Figure 8 Effect of axial dispersion on cycle-averaged feed gas rate. Process conditions are from Murray [4]

5.0 CONCLUSION

The effects of axial dispersion on the numerical simulations of fast cycle adsorption processes were studied using the experimental conditions of Alpay [1] and Murray [4]. Numerical difficulties were encountered when applying Alpay's experimental conditions. The oxygen purity profile for the axial dispersion of 1×10^{-4} m^2 s^{-1} (as in the same order of magnitude calculated using the correlation proposed by Langer *et al.*[11]) reached CSS in an unphysical manner. In contrast to Alpay's experimental conditions, Murray's experimental conditions feature a shorter bed length (L = 0.2 m) and no such numerical difficulties was observed even for plug flow condition. A reduction of up to 10 percentage points in oxygen product purity was obtained with increases in values of axial dispersion coefficients. In future, we plan to look into efficient algorithm to overcome the numerical difficulties encountered in the simulations of 1.0 m column.

ACKNOWLEDGEMENTS

The authors acknowledge the financial support from the Ministry of Science, Environment and Innovation, Malaysia (Project IRPA RMKE 8: 09-02-04-0359-EA001).

NOTATION

dp	particle diameter	m
D	effective axial dispersion coefficient	$m^2\ s^{-1}$
D_e^*	modified effective diffusion coefficient	$m^2\ s^{-1}$
D_m	molecular diffusion coefficient	$m^2\ s^{-1}$
i	an index	
L	length of bed	m
P	total bed pressure	Pa
Pe_∞	limiting value of the Peclet number	
q^*	equilibrium adsorbed phase concentration	$mol\ kg^{-1}$
$\bar{q}$	adsorbed phase concentration averaged over an entire particle volume	$mol\ kg^{-1}$
r_p	radius of an adsorbent particle	m
R_g	ideal gas constant	$J\ mol^{-1}\ K^{-1}$
u	superficial gas velocity	$m\ s^{-1}$
t	time	s
t_c	cycle time	s
T	temperature	K or °C
y	gas phase mole fraction	
z	axial co-ordinate	m

Greek Letters

α	a coefficient in the Ergun equation	
β_{ax}	radial dispersion factor	
ε_b	bed porosity	
ρ_b	bed bulk density	$kg\ m^{-3}$
ρ_g	gas density	$kg\ m^{-3}$
τ_{ax}	axial tortuosity factor	

Subscripts

A, B	component A (oxygen) or component B (nitrogen)
i	component i

Abbreviations

ADPF	axially dispersed plug flow

CSS	cyclic steady state
LDF	linear driving force
OC	orthogonal collocation
ODE	ordinary differential equation
PDE	partial differential equation
RPSA	rapid pressure swing adsorption
TOL	tolerance used in the ODE solver
URPSA	ultra rapid pressure swing adsorption

REFERENCES

[1] Alpay, E. 1992. Rapid Pressure Swing Adsorption Processes. Ph.D. Thesis. University of Cambridge.

[2] Turnock, P. H., and R. H. Kadlec. 1971. Separation of Nitrogen and Methane via Periodic Adsorption. *A.I.Ch.E. J.* 17: 335-342.

[3] Ruthven, D. M., S. Farooq, and K. S. Knaebel. 1994. *Pressure Swing Adsorption*. New York: VCH Publishers.

[4] Murray, J. W. 1996. Air Separation by Rapid Pressure Swing Adsorption. Ph.D. Thesis, University of Cambridge.

[5] Choong, T. S. Y., D. M. Scott, and W. R. Paterson. 1998. Axial Dispersion in Rich, Binary Gas Mixtures: Model Form and Boundary Conditions. *Chemical Engineering Science*. 53: 4147-4149.

[6] Keefer, B. G., and C. R. McLean. 2000. High Frequency Rotary Pressure Swing Adsorption Apparatus. US Patent 6,056,804.

[7] Kulish, S., and R. P. Swank. 1998. Rapid Cycle Pressure Swing Adsorption Oxygen Concentration Method and Apparatus. US Patent 5,827,358.

[8] Alpay, E., C. N. Kenney, and D. M. Scott. 1993. Simulation of Rapid Pressure Swing Adsorption and Reaction Processes. *Chem. Engng Sci.* 48: 3173-3186.

[9] Choong, T. S. Y. 2000. Algorithm Synthesis for Modelling Cyclic Processes: Rapid Pressure Swing Adsorption. Ph.D. Dissertation. University of Cambridge.

[10] Macdonald, I. E., M. S. El-Sayed, K. Mow, and F. A. L. Dullien. 1979. Flow Through Porous Media - the Ergun Equation Revisited. *Ind. Engng. Chem. Fundam.* 18: 199-207.

[11] Langer, G., A. Roethe, K. P. Roethe, and D. Gelbin. 1978. Heat and Mass Transfer in Packed Beds - III. Axial Mass Dispersion. *Int. J. Heat Mass Transfer.* 21: 751-759.

[12] Rice, R. G., and D. D. Do. 1995. *Applied Mathematics and Modelling for Chemical Engineers*. U.S.A.: John Wiley & Sons.

[13] Villadsen, J. V., and M. L. Michelson. 1978. *Solution of Differential Equations by Polynomial Approximation*. New Jersey: Prentice-Hill.

[14] Choong, T. S. Y., D. M. Scott, and W. R. Paterson. 2002. Development of Novel Algorithm Features in the Modelling of Cyclic Processes. *Computers Chem. Engng.* 26: 95-112.

[15] Nilchan, S. 1997. The Optimisation of Periodic Adsorption Processes. Ph.D. Thesis. University of London.

[16] Ko, D., and I. Moon. 2000. Optimization of Start-up Operating Condition in RPSA. *Separation and Purification Technology.* 21: 17-26.